Thermochimica Acta, 10 (1974) 161–176

THE PREPARATION, PROPERTIES, CRYSTAL LATTICE AND THERMAL DECOMPOSITION REACTIONS OF COBALT MALONATE DIHYDRATE

A. K. GALWEY* AND D. M. JAMIESON
Chemistry Department, The Queen's University of Belfast, BT9 5AG (Northern Ireland)
M. LE VAN AND C. BERRO
Chemistry Department, U.E.R.E.P. of Luminy, University of Aix-Marseille (France)

ABSTRACT

Cobalt malonate dihydrate crystallizes in the monoclinic system, the dimensions of the unit cell are reported. On heating, two molecules of water are lost at ~400 K to give the anhydrous salt which is amorphous to X-rays. At higher temperatures (>520 K) the initial stages of carboxylate decomposition obey the zero-order kinetic equation to 30% reaction. Thereafter, there is a marked diminution in rate of the vacuum reaction but kinetic behaviour is sensitive to the gases present; the influences of reaction products, of carbon monoxide and of oxygen have been investigated quantitatively. From these observations we conclude that the decomposition of cobalt malonate proceeds by an autocatalytic mechanism, through the nucleation and growth of an ill-crystallized mixture of product phases. The rate of reactions at the reactant-product contact surface are controlled, to some extent, by available gaseous molecules which may participate in equilibria at the interface and at active surfaces of the residual phases.

INTRODUCTION

Although a voluminous literature reports the results of kinetic and mechanistic investigations of the decomposition reactions of metal carboxylates, formates and oxalates in particular, there is little agreement about the parameters which determine the reactivity of these compounds in the solid state. A particular problem, in making an unambiguous identification of the rate-limiting step for salt breakdown, is the existence of several possible processes which could occupy this role. These include the rupture of one of at least three different bonds in the carboxyl group (–CO–O–M) or alternatively an electron-transfer step or the catalytic rearrangement of an adsorbed species at the surface of a product phase. At the present time no mechanism of carboxylate decomposition has been accorded general acceptance.

*To whom all correspondence should be addressed.

An approach, which could be expected to increase our understanding of these reactions, is through comparisons of behaviour observed for the decomposition of chemically similar reactants. Such studies have been made for many nickel carboxylates but the reactions of the corresponding cobalt compounds have received considerably less attention. A possible reason for this apparently unequal treatment is the somewhat individual (perhaps even unusual) behaviour characteristic of those cobalt salts which have been studied (formate[1], oxalate[2], phthalate[3] and mellitate[4]). The present work on the decomposition of cobalt malonate was undertaken to extend the range of salts of this cation for which kinetic measurements were available. From this it was hoped to identify the factor(s) which controlled, or influenced, the rate of breakdown of these compounds. Another reason for the selection of the malonate was to enable quantitative comparisons to be made with a similar previous study of the reaction of nickel malonate[5]. No report of the pyrolysis of cobalt malonate was found in the literature.

EXPERIMENTAL

Salt decomposition reactions were studied as follows:

(*i*) *Accumulatory conditions.* Measurements[5] were made of the pressure of gas evolved in a constant volume apparatus, a 193 K trap was maintained between reactant and gauge.

(*ii*) *Differential conditions.* Gaseous products were withdrawn[5,6] from the reaction vessel at intervals, using a Toepler pump, and analyzed by gas–solid chromatography.

(*iii*) *Reactions in oxygen.* In the differential apparatus doses of oxygen at equal pressure (40 ± 2 Torr) were admitted to the reactant for a known time interval before removal for product analysis by gas–solid chromatography[6]. Before each kinetic experiment, the reactant was outgassed 2 h at $\sim 10^{-5}$ Torr, prior to heating to the temperature of isothermal (± 1 K) decomposition.

Electron micrographs were obtained using an Akashi TRS-80 instrument. Samples were prepared by a two-stage preshadowed carbon replication technique, shadowing with gold and palladium at $\cot^{-1} 2$.

Preparation of cobalt malonate

Three samples of salt were prepared for study as follows:

Salt A. Freshly precipitated, washed, cobalt hydroxide was dissolved in an aqueous solution of malonic acid and the mixture evaporated for 24 h. The salt obtained was recrystallized.

Salt B. Cobalt carbonate was dissolved in an aqueous solution of malonic acid (10% excess) and heated to 340 K. The precipitate which formed was dissolved, filtered hot and the filtrate evaporated at ambient temperature for 48 h to yield the reactant.

Salt C. Concentrated aqueous solutions of cobalt nitrate and sodium malonate

were mixed. On the addition of excess acetone a viscous liquid separated, which subsequently crystallized and this salt was washed with water, ethanol and ether.

The compositions of all three prepared salts agreed, within experimental accuracy, with the requirements of cobalt malonate dihydrate (Table 1). The weight loss of salt A on dehydration in vacuum, 18.8%, agreed well with that expected for loss of water from the dihydrate (18.28%).

TABLE 1

ANALYTICAL DATA FOR COMPOSITION OF REACTANT SAMPLES

	Salt A	*Salt B*	*Salt C*	*Theoretical* $C_3H_2O_4Co \cdot 2H_2O$
%C (microchemical combustion analysis)	18.28	18.43	18.35	18.30
%H (microchemical combustion analysis)	3.01	3.11	2.99	3.04
%Co (spectroscopic absorption analysis)	29.9	29.7	29.9	29.9

RESULTS

Crystal structure of cobalt malonate dihydrate

The symmetry properties of the unit cell of cobalt malonate dihydrate were determined from single crystal rotation and from Weissenberg X-ray diffraction photographs. Refinement was achieved through a powder diffraction diagram, measured at a low rate of rotation, $1.5'\theta\ \text{min}^{-1}$. We conclude that cobalt malonate dihydrate crystallizes in the monoclinic system and the parameters of the unit cell are (see Appendix):

$a = 12.6793 \pm 0.0038$ Å

$b = 7.4115 \pm 0.0009$ Å

$c = 7.3041 \pm 0.0021$ Å

$\beta = 120.25 \pm 0.02°$

In the absence of a complete structural study we cannot establish the space group from the three possibilities identified: $C2/m$, Cm or $C2$. The density of the salt at 298 K, measured by a picnometric method, was $2.20 \pm 0.07\ \text{g cm}^{-3}$, in good agreement with the theoretical value ($2.21\ \text{g cm}^{-3}$), assuming four molecules per unit cell.

Thermochemical and non-isothermal decomposition measurements

Typical thermogravimetric (TG) and differential thermal analysis (DTA) measurements for salt A are given in Fig. 1. During rapid heating in air (TG at

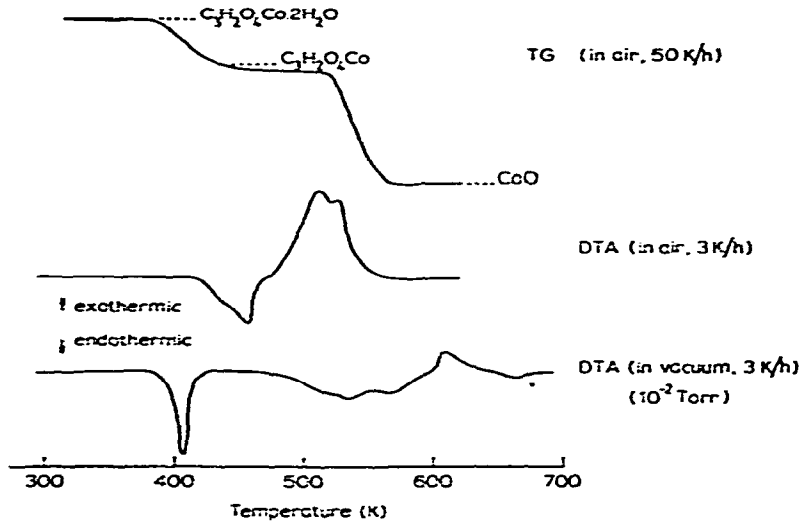

Fig. 1. Representative measurements for the decomposition of cobalt malonate (salt A) under non-isothermal conditions. The weight of the residue from the (relatively rapid, 50 Kh^{-1}) TG in air corresponded to the formation of CoO but the phases present more probably consisted of a mixture of Co, CoO and Co_3O_4 (see text).

50 K h^{-1}) the dehydration reaction was followed by decomposition to yield the oxide product CoO. DTA measurements were made in a Calvet microcalorimeter at the slow heating rate of 3 K h^{-1}. The mean enthalpy of dehydration was 107 ± 4 kJ mol^{-1}, comparable with values measured for very many hydrates[7]. In vacuum, dehydration commenced at a lower temperature (~380 K) than in air (~430 K) but water loss was completed before decomposition started (Fig. 1). The onset of salt breakdown was less sensitive to the presence of gases and commenced at ~490 K, though the heat evolved was somewhat irreproducible and markedly influenced by reaction conditions. In a dynamic vacuum, the heat of the endothermic decomposition reaction was 144 ± 30 kJ mol^{-1}, in argon the value diminished to 12–25 kJ mol^{-1} and in air at 500 K the reaction was significantly exothermic (-110 ± 20 kJ mol^{-1}) to yield a residue which contained metal oxide. The extent of secondary reactions is increased by gases present and the residual products can be oxidized.

Products of decomposition reactions of cobalt malonate

Decomposition of the dehydrated reactant, both under differential and under accumulatory conditions, yielded 1.8 ± 0.1 mol carbon dioxide and 0.3 ± 0.1 mol carbon monoxide per mol of reactant. Appreciable yields of the latter product were detected *only* during the second half of reaction, when α, the fractional reaction, was >0.5. There was complete oxidation of all carbon during decomposition in excess oxygen:

$$C_3H_2O_4Co + 2\tfrac{1}{2}O_2 \rightarrow 3CO_2 + \tfrac{1}{3}Co_3O_4\ (? + H_2O)$$

Identification of all solid phases, other than the prepared crystalline hydrate (salt A), by X-ray diffraction measurements was difficult, since all such materials were poorly crystallized, diffraction peaks were weak and ill-defined. The violet-coloured anhydrous salt was amorphous. The residue from vacuum decomposition of salt A was a mixture in which the phases Co, CoO and Co_2O_3 were identified. The diffraction peaks obtained for the residue from salt B, partially decomposed to $\alpha = 0.2$ and 0.7 in vacuum, were too imprecise to allow the constituent product phases to be recognized. Salt A, partially decomposed to $\alpha = 0.4$ in air, contained CoO, Co_2O_3 and a trace of Co_3O_4. After further reaction, $\alpha > 0.5$, Co_3O_4 was the only crystalline phase detected. We must conclude, therefore, that identification of the solid reaction products is at best qualitative and probably incomplete. We can be sure, however, that residual phases are finely divided and/or poorly crystallized.

Surface areas were determined by the BET method from measurements of the volume of nitrogen adsorbed at 80 K at various equilibrium pressures. The area of salt B after dehydration was 6 $m^2 g^{-1}$ and this increased during decomposition in vacuum to 11 and 33 $m^2 g^{-1}$ at $\alpha = 0.2$ and 0.7, respectively.

Kinetics of decomposition of cobalt malonate

Typical α–time plots for the decomposition of salt A under accumulatory conditions are shown in Fig. 2. An initial, just discernable, deceleratory process ($\alpha < 0.06$) preceded the onset of a zero-order reaction which occurred $0.06 < \alpha < 0.3$.

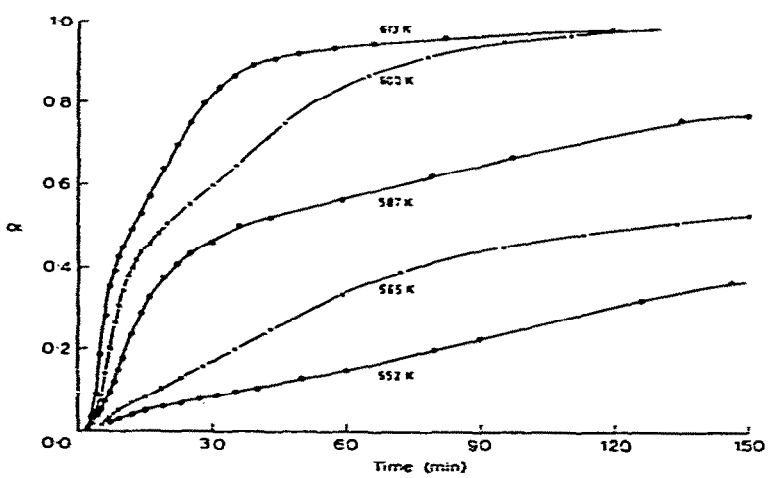

Fig. 2. Typical α–time plots for the thermal decomposition of cobalt malonate (salt A) under accumulatory conditions.

A reduced time plot, Fig. 3, (76 measurements from 7 reactions 572–600 K) confirms that there was no systematic change in reaction rate within this range of α. Subsequently, however, there was a marked reduction in reaction rate between $0.3 < \alpha < 0.45$ and a second period of zero-order kinetic behaviour ($0.45 < \alpha < 0.72$)

preceded the final deceleratory process, during completion of salt pyrolysis. Careful comparison of reduced time data confirmed the existence of a small increase in activation energy from 179 ± 10 kJ mol^{-1} between $0.06 < \alpha < 0.3$ to 183 ± 15 kJ mol^{-1} during the later stages.

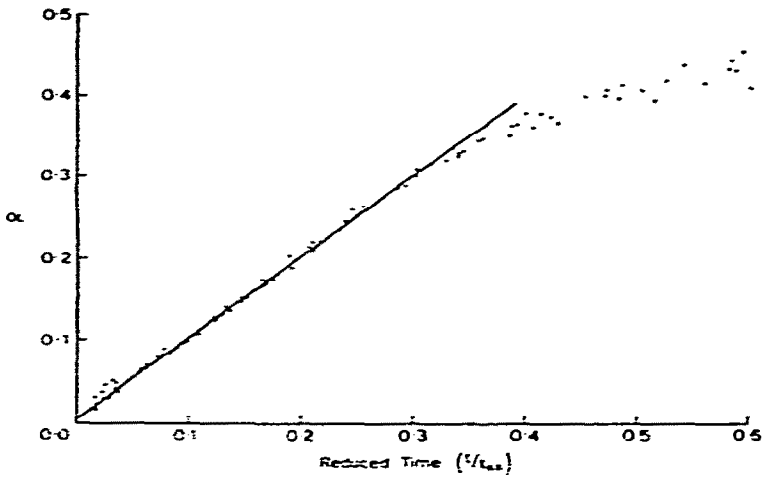

Fig. 3. Reduced-time plot for the initial stages of thermal decomposition of cobalt malonate (salt A) under accumulatory conditions, measurements from seven reactions 572–600 K.

The shape of the α–time curves and the rate of decomposition of salt A were markedly influenced by reaction conditions. Typical behaviour is illustrated in Fig. 4 and quantitative kinetic observations are summarized in Table 2. Unlike cobalt oxalate[2], the rate of decomposition of salt A was independent of whether the reactant sample was previously dehydrated at 420 or at 470 K.

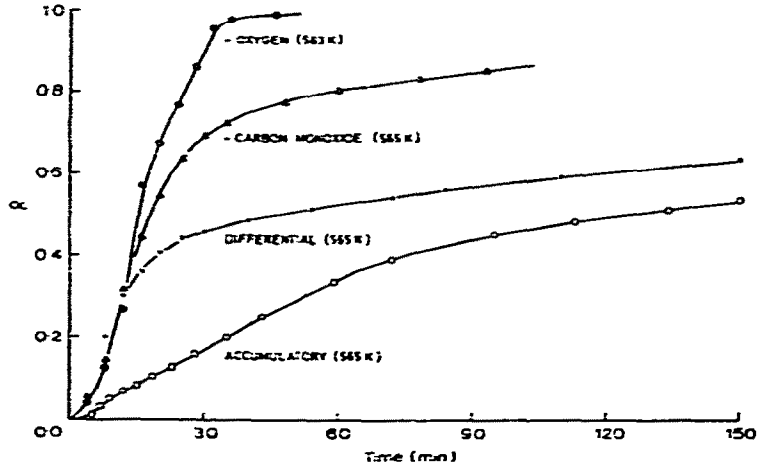

Fig. 4. Comparative α–time plots for the decomposition of cobalt malonate (salt A) under accumulatory and differential conditions and in 40 Torr carbon monoxide or oxygen.

TABLE 2

COMPARATIVE KINETIC DATA FOR THERMAL DECOMPOSITION OF COBALT MALONATE (SALT A) UNDER VARIOUS REACTION CONDITIONS

Reaction conditions	*Value of α at which reaction rate diminished*	*Range of α over which the zero-order kinetic equation was obeyed*	*Relative reaction rate*	*Activation energy (kJ mol^{-1})*	*Temperature interval studied (K)*
Accumulatory	0.4	0.06–0.30	1.0	179 ± 10	572–600
		0.45–0.72	0.2	183 ± 15	
Differential	0.3	0.05–0.30	4	180 ± 12	566–590
In 40 Torr CO	0.5	0.05–0.40	7	179 ± 10	543–563
In 40 Torr O_2	—	0.05–0.5	9	180 ± 12	524–575
		0.6–0.85	—	40 ± 10	

The rate of decomposition of salt A in 40 Torr oxygen remained approximately constant $0.6<\alpha<0.85$ and the apparent activation energy was unexpectedly small (40 kJ mol^{-1}). Thus, at low temperatures (<540 K), the rate of reaction increased when $\alpha>0.6$, at ~540 K there was an approximately constant reaction rate to $\alpha\sim0.9$ and at higher temperatures (>540 K) the rate of reaction diminished when $\alpha>0.6$ (Fig. 5). Since this reaction resulted in complete oxidation of the constituent carbon of the reactant, $\alpha\sim0.65$ corresponds to the point of theoretical completion of the vacuum reaction. In several experiments an oxygen uptake, corresponding to ~0.5 oxygen atom/atom of cobalt in the residue, occurred at $\alpha\sim0.75$. This must be ascribed to oxidation of a solid product, since gas uptake was not accompanied by the

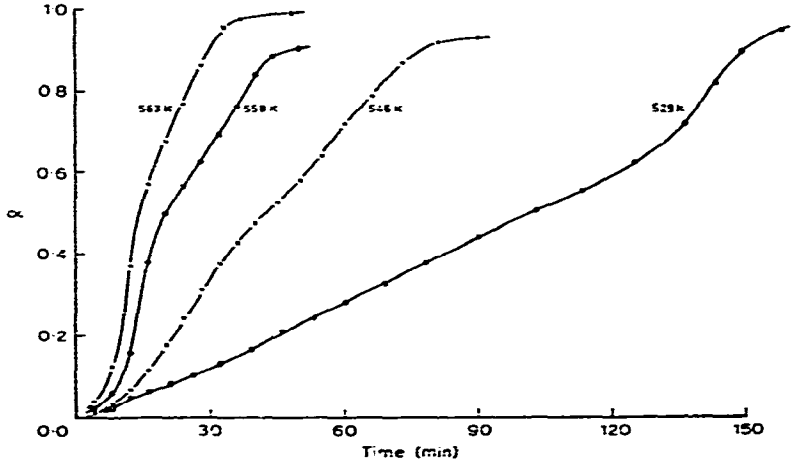

Fig. 5. Typical α–time plots for the thermal decomposition of cobalt malonate (salt A) in 40 Torr oxygen.

evolution of a corresponding volume of carbon dioxide. This observation is consistent with the above evidence from X-ray data that the composition of the residue changes during reaction.

Two samples of salt A were decomposed under accumulatory conditions to completion of the first zero-order process, $\alpha = 0.43$, exposed to water vapour at 293 K for 16 h, returned to the same apparatus and decomposition completed. The shapes of α^1 ($=(\alpha-0.43)/0.57$)–time curves and rate constants for the initial ($0.05<\alpha^1<0.3$) and later ($0.5<\alpha^1<0.6$) periods of reaction were characteristic of decomposition under *differential* conditions. Exposure to water vapour at $\alpha = 0.43$, therefore, increased the reaction rate ($\times 4$) and the rate process between $0.4<\alpha^1<0.7$ was deceleratory.

The shapes of α–time plots and the rates of decomposition of salt B were identical with those for salt A. Crushing or pelleting this reactant caused no change in

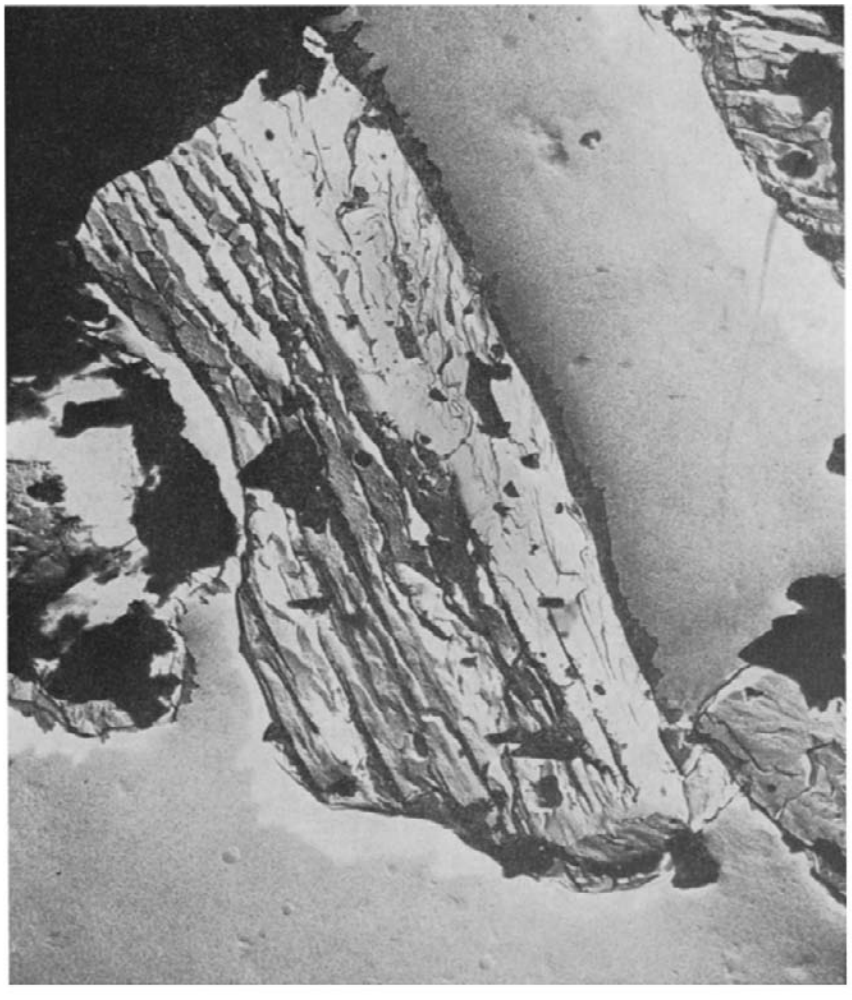

Fig. 6. Surface replica of partially decomposed cobalt malonate (salt A, $\alpha = 0.23$) lightly crushed. ($\times$ 10,600.)

reaction rate. Pressure measurements for the decomposition of salt B, in the accumulatory apparatus using an 80 K trap, showed that gaseous products initially evolved were later converted to condensable materials, following secondary reactions on or with solid products.

The initial rate of decomposition of salt C under accumulatory conditions was greater ($\times 2$) that that of salt A, and there was a small, but detectable, reduction in reaction rate at $\alpha \sim 0.4$. Almost identical shapes of α–time curves were observed for the decomposition of (i) salt C; (ii) salt B, to which 3–5% sodium malonate had been added and the mixture crushed; and (iii) salt A, after interruption of reaction and exposure to water vapour at $\alpha = 0.43$. The kinetic characteristics of salt C were modified by the presence of 2% sodium (measured analytically) retained in this salt preparation and the influence of this impurity was evidently similar to that of water.

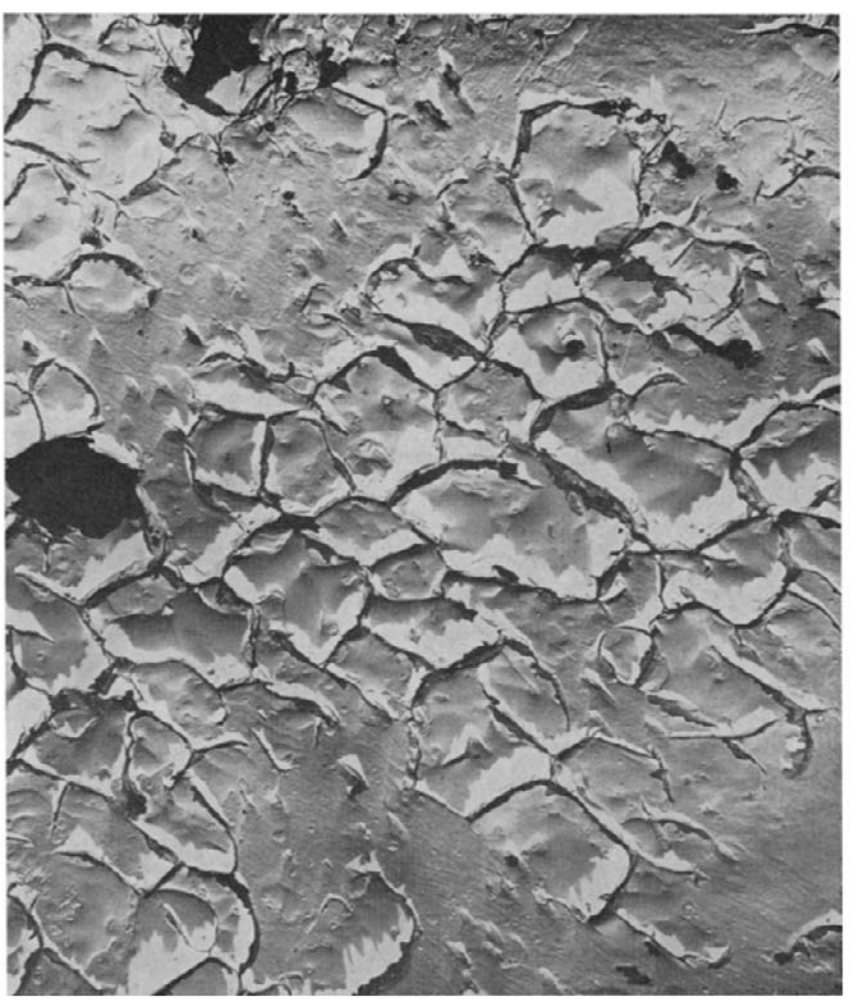

Fig. 7. Surface replica of fully decomposed cobalt malonate (salt A, $\alpha = 1.0$). During decomposition, reaction was interrupted at $\alpha = 0.43$, the salt exposed to water vapour, before reaction proceeded to completion under accumulatory conditions. ($\times 7{,}000$.)

Both additives reduce the diminution in reaction rate at $\alpha \sim 0.4$ and reactions became deceleratory, and not zero order (as in the vacuum reaction), thereafter.

Electron microscopy

Salt A. The surfaces of the prepared dihydrate exhibited a variety of textures: some areas were smooth, other areas were more irregular, containing cracks and/or pits. The appearances of the dehydrated salt ($\alpha = 0.00$), the residual product ($\alpha = 1.00$) and partially decomposed reactant ($\alpha = 0.047$, 0.24, 0.40 and 0.62) were closely comparable; no characteristic surface textural feature was recognized whereby the reactant and product phases could be unambiguously distinguished. Consequently, microscopic observations were not of great importance in the establishment of the reaction mechanism.

Light crushing of partially decomposed salt ($\alpha = 0.23$ and 0.61) revealed internal cracking often, but not invariably, having parallel alignment; a typical

Fig. 8. Surface replica of partially decomposed cobalt malonate (salt B, $\alpha = 0.30$). ($\times$ 7,000.)

structure is shown in Fig. 6. The surfaces of decomposed salt ($\alpha = 1.00$), which had been exposed previously to water vapour at $\alpha = 0.43$, contrasted with the residue from an uninterrupted reaction in possessing an extensive mosaic of surface cracking (Fig. 7).

Salt B. Crystals of this preparation were smaller than those of salt A, the same variety of surface textures were again represented and there was no progressive change during reaction. A small proportion of crystals underwent approximately parallel surface cracking, a representative example is shown in Fig. 8 for salt reacted to $\alpha = 0.3$. After light crushing, or etching with dilute aqueous ammonium hydroxide, the surfaces of salt decomposed at $\alpha = 0.2$ and 0.7 were extensively pitted, indicating the development of an internal pore system during reaction.

DISCUSSION

In general, α–time curves for the isothermal decomposition of cobalt malonate (Figs. 2, 4 and 5) conformed approximately to the sigmoid shape characteristic of solid phase reactions which proceed by a nucleation and growth process. The occurrence of such a mechanism is supported by electron micrographs, in so far as there was no evidence that the reactant particles underwent appreciable sintering or coalescence, though the possibility of local or partial melting cannot be definitely excluded. It was also noted that kinetic behaviour was not characteristic of homogeneous rate processes. Accordingly, we conclude that reaction proceeds by a heterogeneous mechanism and anion breakdown occurs at a reactant-product interface, which progressively advances into undecomposed material. It was not found possible to characterize the topography of this reaction by electron microscopy. Nucleation is not necessarily restricted to external boundary surfaces of the original crystallites but (as in other carboxylate decompositions[8]) also probably occurs at internal surfaces of the disorganized, largely amorphous, material which constituted the dehydrated salt.

The decomposition reaction of cobalt malonate was sensitive to the conditions prevailing (Table 2, Fig. 4 and thermochemical observations), this is not an integral mechanistic feature of reactions which proceed by the nucleation and growth of particles of product phase. We conclude that the reactivity of the mixture of residual phases, including interactions at the reactant-product interface, is sensitive to the gases present. The residual phases, which constitute the growing nuclei, were often amorphous, usually ill-crystallized, invariably difficult to characterize and susceptible to oxidation. In this particular, the present reactant contrasts with behaviour observed in many other decomposition reactions (including nickel carboxylates[5,8]) where crystalline product phases could be readily identified.

Initially ($\alpha < 0.3$) the kinetics of decomposition of cobalt malonate were very closely comparable with behaviour of nickel malonate[5]: a deceleratory reaction (here $\alpha < 0.06$) was followed by a zero-order rate process and the activation energy was 179 kJ mol^{-1}. We conclude, therefore, that reactions proceed by the same

mechanism of growth, through the coalescence of nuclei formed at parallel internal surfaces, and one-dimensional development of product lamellae. This mechanism is supported by the appearance of parallel fissures in the surfaces of partially decomposed reactant (Figs. 6 and 8). The crystal habit of the salt did not, however, exhibit the characteristic twinning found in the nickel salt, and the product phase was less crystalline.

In contrast with these similarities, we note differences in both rate and extent of the initial reactions and in kinetic behaviour when $\alpha > 0.3$ (Table 2), which result from changes in reaction conditions. These differences cannot be positively identified with changes in the geometry of progression of the reaction interface and are ascribed to participation by gases present in rate processes at the reactant-product contact surface.

Comparisons between the decomposition reactions of the salt in vacuum and in oxygen showed that under the latter conditions the rate of product evolution was relatively greater, there was no marked diminution at $\alpha \sim 0.3$, or subsequently as reaction proceeded to completion, and products were more highly oxidized. We suggest that these differences result from deposition of carbon at the reaction interface during decomposition in vacuum, so restricting development, but this inhibiting barrier phase (or poison) is converted to carbon dioxide when excess oxygen is available. The vacuum reaction yielded a finely divided, ill-crystallized residue, probably containing Co, CoO and Co_2O_3, but, though carbon was present, no crystalline phase containing this element could be recognized. The metal carbide (a residual product in the decomposition of the nickel salt[5]) was not identified, probably because the rate of decomposition of cobalt carbide[9] at 600 K is only slightly less than that of the malonate. Carbon deposited at the interface reduces the reaction rate at $\alpha = 0.3$ but subsequently the inhibited reaction again obeyed the zero-order equation ($0.45 < \alpha < 0.72$) and the activation energy was just perceptibly increased. The reactions of oxygen with the salt and/or products varied as reaction proceeded. Initially the decomposition rate of the salt was accelerated, the characteristic diminution at $\alpha = 0.3$ was absent but the zero-order behaviour and activation energy were unaltered. Reactant oxidation during the initial stages was, however, incomplete since there was a large uptake of gas at $\alpha \sim 0.75$ (not accompanied by carbon dioxide evolution and after a yield corresponding to the theoretical completion of the vacuum decomposition). The change of solid product and mechanism $\alpha > 0.6$ accounts for the thermochemical observations (Fig. 1) and the unexpectedly small activation energy.

The most significant difference between conditions which obtain during accumulatory and differential reactions is in the availability of water vapour: there was no refrigerent trap in the differential apparatus. It appeared possible, therefore, that the participation of water at the reaction interface accelerated decomposition. To test this hypothesis, kinetic studies were made of the decomposition of partially reacted salt, following exposure to water vapour at $\alpha = 0.43$, under accumulatory conditions. The subsequent kinetic behaviour of this reactant was characteristic of

reactions proceeding under *differential* conditions. The common parameter in both experiments was the availability of water which must, therefore, facilitate reaction. Furthermore, this effect closely resembled that found on addition of sodium malonate to salt B or this impurity in salt C. The incorporation of monovalent ions (OH^-, H^+ or Na^+) in the reactant may be expected to confer mobility on the constituents of pure cobalt malonate, which contains divalent species only, disposed in an amorphous (to X-rays) assemblage. The additional defects envisaged resemble those postulated to control the reactivity of silver carbonate[10]. The consequent facilitation of lattice reorganization of the reactant influences equilibria and conditions at the reactant-product contact interface so that there is an increase in rate of salt decomposition.

The experiment in which evolved carbon monoxide underwent a secondary reaction to yield condensable (at 80 K) products demonstrates the reactivity or catalytic properties of the residual phases and the participation of this gaseous product in surface processes. Indeed, the appearance of this product only after $\alpha > 0.5$ is an indication of the complexity of the chemical interactions and the progressive variation in interface properties as reaction proceeds. The influence of excess carbon monoxide on reaction rate (Table 2) is, therefore, ascribed to participation in surface equilibria, under conditions which do not ensure the irreversible and rapid removal of water.

CONCLUSIONS

From the above discussion, we conclude that a reaction mechanism based on the nucleation and growth of a single product phase does not provide a complete description of the thermal decomposition of cobalt malonate. There is strong evidence that gaseous species, notably oxygen, water and probably carbon monoxide, participate in the sequence of steps which result in carboxylate breakdown. Therefore, in addition to the dependence of reaction rate on geometric factors, some control also derives from the influence of chemisorbed species on surface equilibria and participation of the gases present in the rate-controlling step at the reactant-product interface. As a consequence, kinetic behaviour is sensitive to prevailing conditions, and, in particular, the availability of volatile reactive molecules. There was a progressive increase in reaction rate, by almost an order of magnitude (Table 2), with increase in reactivity of gases present. The effect of these gases, during the early stages of reaction, is apparently restricted to an influence on the Arrhenius pre-exponential term (Table 2): this is readily ascribed to participation of gases in interface equilibria. Subsequent behaviour is believed to result from the surface reactivity and the surface properties of the solid products including interaction with deposited carbon at the reactant-product contact. The dependence of kinetic behaviour on gaseous atmosphere became more pronounced when $\alpha > 0.3$.

The decomposition of cobalt malonate resembles the reactions of other cobalt carboxylates[1–4] in exhibiting a pattern of kinetic behaviour which differs from that of the corresponding nickel salt. The present reactant resembles nickel malonate to some extent when $\alpha < 0.3$ but, thereafter, significant differences are apparent. We ascribe

these variations to the properties and reactivity of the solid product phases which are less crystalline and more reactive with gases present than those of the nickel salts. Similar considerations are probably applicable to other cobalt carboxylates. We conclude that difficulties in establishing the chemistry of reactions occurring at the reactant-product interface in cobalt salts are a consequence of the ill-defined and variable compositions of the active surfaces of the product phases which participate in autocatalytic reactions. Significantly, cobalt forms more than one stable oxide. Further advance in the understanding of these processes necessitates more detailed knowledge of the structure and properties of these mixtures of product phases. The complexity of the interface phenomena makes it impracticable to speculate about the nature of the rate-limiting step at present, but clearly more than one such step may well be involved in the various reactions described here.

ACKNOWLEDGEMENTS

We thank Mr. R. Reed and Mr. T. Conway, of the Electron Microscopy Unit, Q.U.B., for assistance in obtaining and interpreting electron micrographs. D. J. thanks the Ministry of Education for Northern Ireland for a postgraduate award.

REFERENCES

1 G. Perinet and M. Le Van, *C. R. Acad. Sci. (Paris), Ser. C*, 266 (1968) 201.
2 D. Broadbent, D. Dollimore and J. Dollimore, *J. Chem. Soc. A*, (1966) 1491.
3 R. J. Acheson and A. K. Galwey, *J. Inorg. Nucl. Chem.*, 30 (1968) 2383.
4 A. K. Galwey, *J. Chem. Soc. A*, (1966) 87; R. J. Acheson and A. K. Galwey, *J. Chem. Soc. A*, (1968) 1125.
5 K. A. Jones, R. J. Acheson, B. R. Wheeler and A. K. Galwey, *Trans. Faraday Soc.*, 64 (1968) 1887.
6 A. K. Galwey, *J. Catal.*, 1 (1962) 227.
7 M. Le Van, *Bull. Soc. Chim. Fr.*, (1972) 579.
8 M. J. McGinn, B. R. Wheeler and A. K. Galwey, *Trans. Faraday Soc.*, 66 (1970) 1809.
9 L. J. E. Hofer, M. E. Cohn and W. C. Peebles, *J. Phys. Colloid Sci.*, 53 (1949) 661.
10 P. A. Barnes and F. S. Stone in J. W. Mitchell (Ed.), *Reactivity of Solids*, Vol. 6, Wiley-Interscience, New York, 1969, p. 261.

APPENDIX

TABLE OF LATTICE SPACINGS FOR COBALT MALONATE DIHYDRATE ($CH_2(CO_2)_2Co \cdot 2H_2O$)

Comparison of calculated lattice spacings with measured X-ray diffraction data. The relative intensities are compared on the scale: vS > S > m > mw > w > vw > vvw.

The extinction laws: *h*, *k*, *l*: $h+k=2n$; *h*, 0, *l*: $(h=2n)$; 0, *k*, 0: $(k=2n)$ correspond to the space groups: *C* 2/*m*, *Cm*, *C*2.

h	*k*	*l*	d_{calc} (Å)	d_{obs} (Å)	I_{obs}
0	0	1	6.310	—	vvw
1	1	0	6.138	6.152	vw
−2	0	1	5.842	5.853	w

(*Continued on p. 175*)

TABLE (*continued*)

h	*k*	*l*	d_{calc} (Å)	d_{obs} (Å)	I_{obs}
2	0	0	5.477	5.482	m
−1	1	1	5.193	5.208	vS
1	1	1	3.886	3.894	S
0	2	0	3.706	3.708	w
−3	1	1	3.661	3.659	mw
−2	0	2	3.639	3.639	
2	0	1	3.378	3.381	S
3	1	0	3.275	3.273	w
−1	1	2	3.197	3.198	vw
0	2	1	3.195	—	
−4	0	1	3.160	—	vw
0	0	2	3.155	3.153	
−2	2	1	3.129	3.129	w
2	2	0	3.069	—	w
−3	1	2	3.068	3.068	
−4	0	2	2.921	2.918	w
4	0	0	2.738	—	vvw
−2	2	2	2.597	2.597	vw
1	1	2	2.531	2.532	vw
2	2	1	2.497	2.497	mw
3	1	1	2.484	2.485	mw
−2	0	3	2.412	—	w
1	3	0	2.410	—	
−4	2	1	2.404	2.404	
0	2	2	2.402	—	
−5	1	1	2.365	2.363	vvw
−5	1	2	2.349	—	vvw
−1	3	2	2.339	2.339	vw
−4	0	3	2.328	2.328	vw
−3	1	3	2.306	2.307	w
−4	2	2	2.294	2.293	w
2	0	2	2.281	2.284	w
4	2	0	2.202	2.202	w
−1	1	3	2.188	—	
1	3	1	2.173	2.174	vvw
4	0	1	2.148	2.147	vvw
−3	3	1	2.131	2.131	vw
−6	0	2	2.105	—	vvw
0	0	3	2.103	—	
5	1	0	2.101	2.101	
−5	1	3	2.067	2.066	vw
−6	0	1	2.051	—	vw
3	3	0	2.046	2.046	
−1	3	2	2.027	2.027	vvw
−2	2	3	2.021	—	
−3	3	2	1.993	1.993	vw
−4	2	3	1.971	1.972	vvw
−6	0	3	1.947	—	vvw
2	2	2	1.943	1.944	vw

(*Continued on p. 176*)

TABLE (*continued*)

h	k	l	d_{calc} (Å)	d_{obs} (Å)	I_{obs}
3	1	2	1.886	1.885	vvw
4	2	1	1.858	—	vw
0	4	0	1.853	1.853	
1	1	3	1.837	1.837	vvw
−6	2	2	1.831	—	vvw
0	2	3	1.829	—	
6	0	0	1.826	1.827	
1	3	2	1.820	—	
−4	0	4	1.820	—	
3	3	1	1.803	1.802	vvw
−6	2	1	1.794	—	vvw
0	4	1	1.778	—	vvw
−2	0	4	1.772	1.771	
−3	1	4	1.767	—	vvw
−2	4	1	1.766	—	
−7	1	2	1.759	—	vw
−5	3	1	1.756	—	
5	1	1	1.755	—	
2	4	0	1.755	—	
−5	3	2	1.749	—	vvw
−3	3	3	1.731	—	vvw